TESTING FOR ANCIENT ADAPTIVE RADIATIONS IN NEOTROPICAL CICHLID FISHES

Hernán López-Fernández,[1,2,3] Jessica H. Arbour,[2] Kirk. O. Winemiller,[4] and Rodney L. Honeycutt[5]

[1]Department of Natural History, Royal Ontario Museum, 100 Queen's Park, Toronto, Ontario M5S 2C6, Canada

[2]Department of Ecology and Evolutionary Biology, University of Toronto, 25 Willcocks St., Toronto, Ontario M5S 3B2, Canada

  [3]E-mails: hernanl@rom.on.ca, hlopez_fernandez@yahoo.com

[4]Section of Ecology, Evolution and Systematic Biology, Department of Wildlife and Fisheries Sciences, Texas A&M University, College Station, Texas 77843

[5]Natural Science Division, Pepperdine University, 24255 Pacific Coast Hwy., Malibu, California 90263

Most contemporary studies of adaptive radiation focus on relatively recent and geographically restricted clades. It is less clear whether diversification of ancient clades spanning entire continents is consistent with adaptive radiation. We used novel fossil calibrations to generate a chronogram of Neotropical cichlid fishes and to test whether patterns of lineage and morphological diversification are congruent with hypothesized adaptive radiations in South and Central America. We found that diversification in the Neotropical cichlid clade and the highly diverse tribe Geophagini was consistent with diversity-dependent, early bursts of divergence followed by decreased rates of lineage accumulation. South American Geophagini underwent early rapid differentiation in body shape, expanding into novel morphological space characterized by elongate-bodied predators. Divergence in head shape attributes associated with trophic specialization evolved under strong adaptive constraints in all Neotropical cichlid clades. The South American Cichlasomatini followed patterns consistent with constant rates of morphological divergence. Although morphological diversification in South American Heroini was limited, Eocene invasion of Central American habitats was followed by convergent diversification mirroring variation observed in Geophagini. Diversification in Neotropical cichlids was influenced by the early adaptive radiation of Geophagini, which potentially limited differentiation in other cichlid clades.

KEY WORDS: Diversification, ecological opportunity, ecomorphology, fossil calibration, relaxed molecular clock.

Adaptive radiation is a major force generating biodiversity (Simpson 1953; Schluter 2000; Glor 2010). With some recent exceptions (e.g., Claramunt 2010; Derryberry et al. 2011; Claramunt et al. 2012), most contemporary studies of adaptive radiation have focused on relatively recent events in restricted biogeographic areas (Baldwin 1997; Verheyen et al. 2003; Grant and Grant 2008; Losos 2009; Takahashi and Koblmüller 2011). Is it possible to identify adaptive radiations within ancient clades with extant taxa spread across entire continents? Glor (2010) warns "the hierarchical nature of evolutionary diversification makes it increasingly difficult to diagnose adaptive radiation as we move deeper into the tree of life." Recent methods to estimate divergence times from molecular phylogenies and to test models of lineage and phenotypic diversification on chronograms provide powerful tools for studying radiations that occurred deep in time and encompassing vast regions (Rabosky 2009a; Burbrink and Pyron 2010; Mahler et al. 2010).

In adaptive radiations, bursts of lineage diversification are accompanied by a concordant increase in diversification into vacant ecological niches (Simpson 1953; Harmon et al. 2003;

Glor 2010) available through "ecological opportunity," a prerequisite of adaptive radiation (Schluter 2000; Losos 2010; Yoder et al. 2010). Recent reviews (Gavrilets and Losos 2009; Glor 2010) listed a series of patterns that characterize adaptive radiations, at least three of which can be detected with phylogeny-based comparative methods: (1) early bursts of lineage diversification, (2) subsequent decrease in lineage diversification or "overshooting" from decreased speciation and/or increased extinction rates, and (3) subsequent decrease in rates of phenotypic evolution (Harmon et al. 2003; Gavrilets and Losos 2009). The first two patterns together are interpreted as evidence of diversity-dependent or ecological regulation of lineage diversification as increasingly reduced niche availability limits the number of successfully established lineages (Rabosky 2009a,b; Losos 2010). The third pattern can be used to identify an adaptive burst through phylogenetic analyses of phenotypic disparity. Ecological opportunity can be difficult to estimate, but in the absence of a direct metric, disparity of ecologically relevant traits provides a meaningful proxy for ecological opportunity at the time of divergence (Mahler et al. 2010). This approach also allows evaluation of whether phenotypic diversification in certain clades is extraordinary, a requisite for adaptive radiations according to some definitions (Losos and Mahler 2010).

Despite extensive research on East African cichlid adaptive radiations (e.g., Kornfield and Smith 2000; Kocher 2004), little is known about the evolution of cichlids inhabiting rivers of the Neotropics, a species-rich group encompassing remarkable morphological, ecological, and behavioral diversity. Neotropical cichlids (subfamily Cichlinae) are a monophyletic group (Stiassny 1991; Farias et al. 2000; Sparks and Smith 2004) sister to African cichlids. Cichlinae ranges from northern Argentina to Texas and the Caribbean, with more than 600 known species (Kullander 2003). Most Neotropical cichlid diversity is distributed among the major tribes Geophagini, Heroini, and Cichlasomatini (López-Fernández et al. 2010). Geophagini is a South American clade with over 300 species, displaying remarkable ecomorphological and behavioral diversification. Many geophagines are morphologically and behaviorally specialized for substrate-sifting within the oropharyngeal chamber, separating benthic invertebrates from sandy or silty substrates (López-Fernández et al. 2012). Heroini includes about 150 mostly Central American species with significant morphological diversification and specialized trophic niches, including substrate-sifting invertivores, piscivores, detritivores, and frugivores, some of which converge with their South American geophagine counterparts (Winemiller et al. 1995). Cichlasomatini, with over 70 mostly South American species is less ecomorphologically diverse than the other two tribes.

Phylogenetic analyses of Cichlinae suggest divergence of Geophagini and Heroini and to a lesser extent of Cichlasomatini through early adaptive radiation (López-Fernández et al. 2005,

2010). Ecomorphological diversification may also have occurred early in the history of Geophagini (López-Fernández et al. 2012), and recent fossil evidence indicates that some extant lineages originated before the Eocene (e.g., †*Gymnogeophagus eocenicus*, Malabarba et al. 2010). No agreement exists regarding the age of cichlids, as some estimates are consistent with current phylogenetic hypotheses (Stiassny 1991; Sparks & Smith 2004) congruent with Gondwanan origins (Genner et al. 2007; Azuma et al. 2008), and others support much younger ages (e.g., Murray 2001; Santini et al. 2009; Near et al. 2012). Disagreement likely results from a scarce fossil record and variations in the use of calibrations and methods for age estimation with molecular phylogenies (e.g., Ho 2007; Dornburg et al. 2012; Near et al. 2012; Parham et al, 2012; Lukoschek et al. 2012).

In this article we use newly described South American cichlid fossils to calibrate a multilocus phylogeny of Neotropical cichlids (López-Fernández et al. 2010). We provide new estimates of cichlid divergence times and interpret them in the context of assumptions underlying prior estimates of cichlid age. We use the resulting chronogram to test whether patterns of lineage and morphological diversification within Cichlinae and each of its three main tribes are congruent with expectations from adaptive radiation. We focus our analyses on higher-level diversification among Neotropical cichlids and use models of lineage accumulation and phenotypic divergence to test if (1) Neotropical cichlids show evidence of early bursts of lineage diversification followed by a decrease in rates of divergence, and (2) there are detectable shifts in rates of morphological evolution during the evolutionary history of Cichlinae. Our results indicate that an important portion of Neotropical cichlid diversity originated through ancient, continent-wide adaptive radiation.

Methods
PHYLOGENY OF THE NEOTROPICAL CICHLIDAE AND DIVERGENCE TIMES

We used the phylogeny from López-Fernández et al. (2010) to estimate times of divergence and test hypotheses of lineage and phenotype patterns of diversification in Neotropical cichlids. The phylogeny was derived from 3868 aligned base pairs of DNA sequences from three mitochondrial genes and two nuclear loci from 166 cichlid terminals, including 160 Neotropical taxa. All recognized genera of Neotropical cichlids were represented by at least one species. Details of loci, PCR primers and profiles, alignment, and GenBank accession numbers are given in López-Fernández et al. (2010).

Using the same unlinked models of nucleotide substitution as López-Fernández et al. (2010), we estimated divergence times based on relaxed molecular clock methods (Drummond et al.

2006) implemented in BEAST 1.6.2 (Drummond and Rambaut 2007). Times were calculated under an uncorrelated Log-normal tree prior with a Yule prior on speciation. Time calibrations were constrained on three nodes using recently described South American cichlid fossils representing crown-group lineages of each of the three major Neotropical cichlid tribes Geophagini, Cichlasomatini, and Heroini. Two of the calibrations, the geophagine fossil †*Gymnogeophagus eocenicus* (Fig. 1, Node 1, Malabarba et al. 2010) and the heroine †*Plesioheros chauliodus* (Fig. 1, Node 3, Alano-Pérez et al. 2010) were dated to approximately 49 Ma (Malabarba et al. 2010). The third calibration was the cichlasomatine fossil †*Tremembichthys garciae* (Fig. 1, Node 2, Malabarba and Malabarba 2008), with an approximate age of 34 Ma (Alano-Pérez et al. 2010). Fossil calibrations were enforced using exponential priors with a hard-bound minimum age corresponding to the estimated age of the fossils (Table 1). We also used a normally distributed prior (mean = 143.0 Ma, SD = 13.4) for the root age of the cichlid tree based on the time of separation of eastern and western Gondwana (Africa-Madagascar, 121.0–165.0 Ma; Rabinowitz et al. 1983; Genner et al. 2007). Fossil-calibrated exponential priors were constrained such that the upper bound 95% highest posterior density (95% HPD) value coincided with the mean of the root height prior at 143 Ma (Table 1). Further details on the age, provenance and phylogenetic placement of fossil calibrations and of the root prior are in Appendix S1.

Two separate MCMC searches of 200×10^6 iterations were initiated from a random tree, and convergence of the searches was evaluated using Tracer v.1.5 (Drummond and Rambaut 2007). Each MCMC chain was sampled every 20,000 iterations, generating 10,000 chronograms, of which 3,000 were discarded as burn-in and the remaining 7,000 were used to: (a) calculate a maximum clade credibility (MCC) chronogram and corresponding 95% HPD intervals, and (b) randomly sample 1,000 chronograms to use in hypothesis testing of lineage end phenotype diversification.

We obtained additional sets of MCC and 1000-chronogram sets for each major clade of Neotropical cichlids (Geophagini, Cichlasomatini, Heroini) by pruning the original MCC and chronograms obtained from BEAST. Finally, we scaled all trees to a total length of 1 to allow for direct comparisons across phylogenies in all the lineage and phenotypic diversification analyses described later.

RATES AND PATTERNS OF LINEAGE DIVERSIFICATION

We studied patterns of lineage diversification within Cichlinae (Neotropical cichlids) and its main three clades by implementing models of speciation and lineage accumulation through time. Because some metrics of lineage diversification are known to be

sensitive to both taxon sampling (Pybus and Harvey 2000) and recent but unaccounted for diversification events (i.e., young splits not yet recognized as distinct species or otherwise unrecognized diversity; Fordyce 2010), we attempted to reduce possible biases by truncating the most recent one third of each chronogram before performing gamma statistic and lineage diversification model fitting analyses. Truncation ages for each clade were calculated from the dates obtained in this study as follows: Cichlinae = 41.5 Ma, Geophagini = 35.6 Ma, Cichlasomatini = 27.2 Ma, and Heroini = 25.5 Ma.

Lineage through time (LTT) plots for each set of MCC and 1,000 chronograms were produced to graphically summarize trends of lineage accumulation in each tree, but we restricted our interpretations to the earlier two thirds of the chronogram's length to avoid the biases described earlier. We used the gamma statistic from truncated chronogram sets (Pybus and Harvey 2000) to determine whether a signal of decreased diversification was detectable in either Cichlinae or any of three main subclades. To study patterns of lineage accumulation and possible rate change through time in each phylogeny, we fitted two constant-rate and three variable-rate models of lineage diversification. We tested whether the best-fitting model of lineage accumulation in any of the clades was diversity dependent as expected in an ecology-driven diversification process (Rabosky 2009a,b). Under diversity-dependent models, diversification rates are expected to decrease continually over time following either an exponential (DDX) or a linear (DDL) model (Rabosky and Lovette 2008). These models were compared with a nondiversity dependent rate-variable model with instantaneous rate change (Yule-2-rate). All three variable rate models were compared to a pure-birth and a birth–death model with constant rate of lineage accumulation.

We used the sample-size corrected Akaike Information Criterion (AICc) to evaluate support for each of the five models of lineage diversification (Table 2) by comparing ∆AIC values as per Burnham and Anderson (2002). We compared the probability that each model represents the best model using the Akaike weight, or weight of evidence for each model on the MCC trees and the average Akaike weight across all sets of 1000 trees for each clade. When a single model was not clearly preferred, we considered support for all models with either fixed or variable rates by examining the cumulative Akaike weights across these models (Burnham and Anderson 2002).

RATES AND PATTERNS OF PHENOTYPIC DIVERGENCE
We gathered a dataset of eight morphometric attributes and standard length (SL) in preserved museum specimens to represent characters of known correlation with ecology (Winemiller et al. 1995; López-Fernández et al. 2012). Morphological measurements included: (1) head length, measured from the tip of the
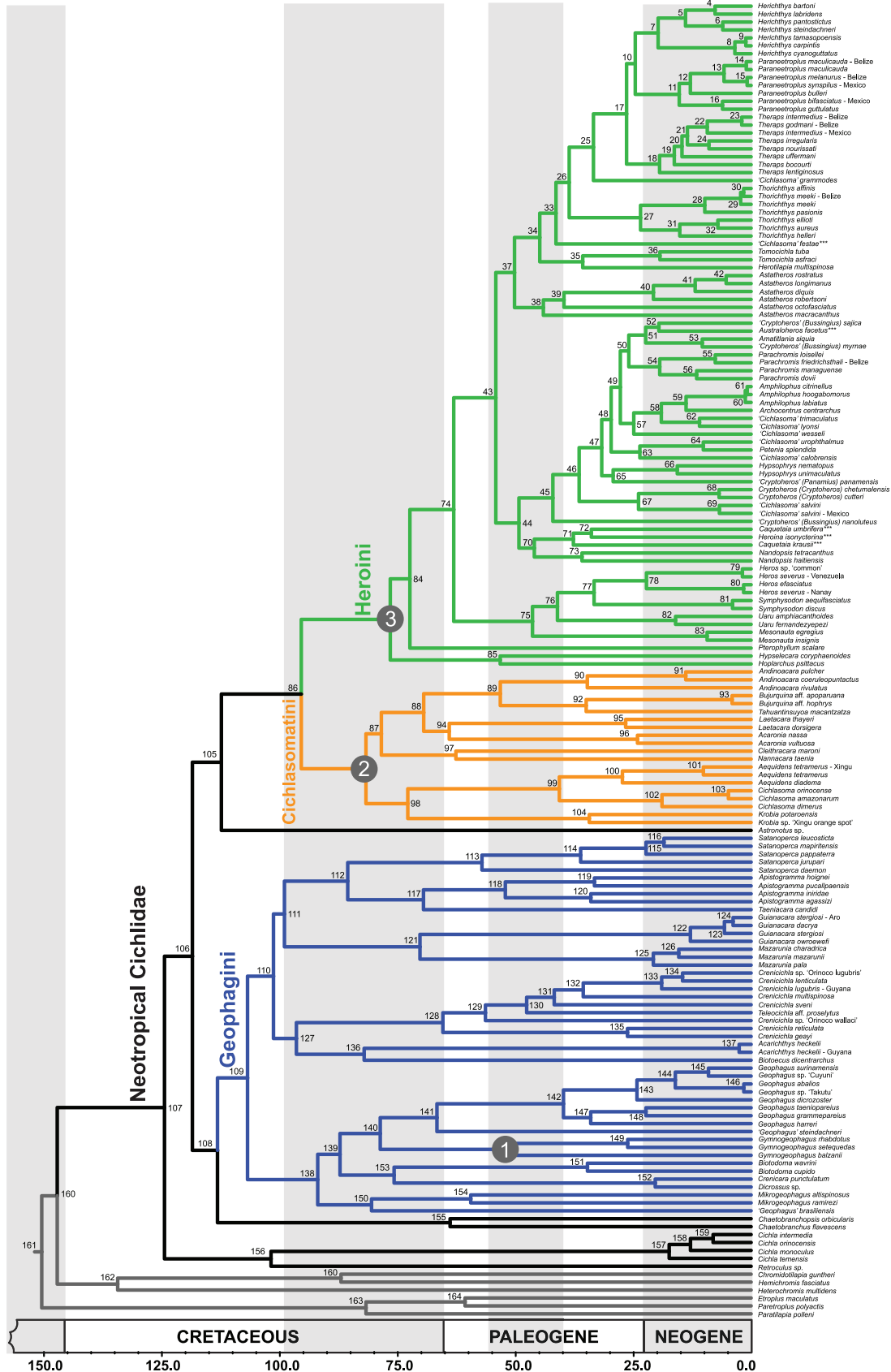
Figure 1.

Table 1. Calibration points and exponential prior distribution parameters used in the BEAST analyses of divergence times.

| Calibration Point | Clade | Minimum age (Ma) | BEAST Calibration Parameters | | | |
			Minimum age bound type	Maximum age bound type	Mean	95% HPD
†*Tremembichthys garciae*[1]	Cichlasomatini	34.0	Hard	Soft	36.4	35.9–143.0
†*Gymnogeophagus eocenicus*[2]	*Gymnogeophagus* (Geophagini)	49.0	Hard	Soft	31.4	50.6–143.1
†*Plesioheros chauliodus*[3]	Heroini	49.0	Hard	Soft	31.4	50.6–143.1

[1]Malabarba and Malabarba 2008, [2] Malabarba et al. 2010, [3] Alano Pérez et al. 2010

Table 2. Comparison of models of lineage accumulation based on the MCC and 1000 chronogram set for each clade.

Clade	Model	$\log(L)_{MCC}$	ΔAIC_{MCC}	$AICweight_{MCC}$	$\log(L)_{1000}(SD)$	$\Delta AIC_{1000}(SD)$	$AICweight_{1000}(SD)$
Cichlinae	Pure birth	−155.50	3.13	0.09	−168.13 (19.92)	2.96 (2.13)	0.13 (0.08)
	Birth–death	−155.50	5.13	0.03	−168.13 (19.92)	4.96 (2.13)	0.05 (0.03)
	DDX	−158.06	0.00	0.43	−170.36 (19.72)	0.50 (0.82)	0.34 (0.11)
	DDL	−157.69	0.73	0.30	−169.58 (19.52)	2.07 (1.34)	0.16 (0.08)
	Yule-2-Rate	−157.97	2.17	0.15	−171.30 (19.86)	0.63 (0.73)	0.33 (0.14)
Geophagini	Pure birth	−58.70	4.90	0.05	−60.43 (6.94)	5.92 (2.54)	0.04 (0.04)
	Birth–death	−58.70	6.90	0.02	−60.43 (6.94)	7.92 (2.54)	0.02 (0.02)
	DDX	−62.15	0.00	0.54	−64.14 (6.50)	0.50 (0.95)	0.41 (0.14)
	DDL	−61.44	1.43	0.26	−63.28 (6.22)	2.23 (1.80)	0.21 (0.14)
	Yule-2-Rate	−61.75	2.80	0.13	−64.79 (6.70)	1.20 (1.20)	0.32 (0.18)
Cichlasomatini	Pure birth	−18.40	0.91	0.22	−17.52 (3.64)	2.57 (2.03)	0.14 (0.09)
	Birth–death	−18.40	2.91	0.08	−17.52 (3.65)	4.56 (2.03)	0.05 (0.05)
	DDX	−19.85	0.00	0.34	−19.58 (3.24)	0.43 (0.86)	0.35 (0.12)
	DDL	−18.99	1.73	0.14	−18.98 (3.12)	1.64 (1.35)	0.2 (0.12)
	Yule-2-Rate	−20.40	0.91	0.22	−20.15 (3.49)	1.31 (1.21)	0.24 (0.14)
Heroini	Pure birth	82.31	0.00	0.27	−88.07 (13.73)	0.68 (1.35)	0.29 (0.11)
	Birth–death	82.31	2.00	0.10	−88.10 (13.72)	2.62 (1.39)	0.11 (0.05)
	DDX	82.68	1.26	0.14	−88.49 (13.79)	1.83 (0.89)	0.15 (0.04)
	DDL	83.24	0.15	0.25	−88.78 (13.74)	1.26 (0.83)	0.21 (0.07)
	Yule-2-Rate	84.20	0.23	0.24	−89.80 (13.71)	1.21 (1.05)	0.23 (0.14)

upper lip with the mouth closed to the caudal edge of the operculum; (2) head height, the vertical distance through the center of the eye, between the dorsal and ventral edges of the head; (3) eye position, the vertical distance between the center of the eye and the ventral edge of the head; (4) eye diameter, the longest horizontal distance between the anterior and posterior edges of the eye; (5) snout length, the distance from the center of the eye to the center of the upper lip; (6) body depth, vertically at the highest point of the body; (7) caudal peduncle depth, vertically from dorsal to ventral edge of the peduncle at mid-length; and (8) gape width, the horizontal internal distance between the tips of the premaxilla with the mouth open.

Figure 1. A chronogram of Cichlinae based on the multilocus phylogeny presented by López-Fernández et al. (2010) and three fossil calibration points (nodes 1–3). Lineages represent all clades and currently recognized genera within Neotropical cichlids. Posterior probabilities, age means, and 95% HPD values for all nodes are given in Appendix S2 following node numbers in this figure. The three clades highlighted in colors represent each of the major tribes within Cichlinae, Blue = Geophagini, Orange = Cichlasomatini, Green = Heroini, respectively. Nomenclature follows López-Fernández et al. (2010).

Our dataset included 575 preserved specimens representing 1 to 8 individuals for 127 (82%) species of Neotropical cichlids present in the López-Fernández et al. (2010) phylogeny. We only measured adult specimens to reduce biases introduced by allometry. All measurements were performed by HLF using digital calipers to the nearest 0.1 mm. We also created a maximum body-size dataset for 143 species (92.8% of species in López-Fernández et al. [2010] phylogeny) gathered from Reis et al. (2003) and FishBase (Froese and Pauly 2011). If our measurements revealed larger specimens than those available in the literature, we replaced published records with our data. Specimens evaluated for body size are cataloged at the Museo de Ciencias Naturales de Guanare, Venezuela, or the Royal Ontario Museum, Canada. We natural log-transformed the data and calculated mean values for each trait to characterize each species.

We corrected species values for phylogenetic history and size variation by performing regression of each morphological variable against SL using phylogenetic size correction with the "phyl.resid" function from the phytools R package (Revell 2012). Phylogenetic principal components analysis (PCA) was performed on the eight morphological traits using a correlation matrix, which is similar to phylogenetic size correction and accounts for nonindependence of species trait values (Revell 2009). We considered critical PC axes (representing nonrandom variation) as those with eigenvalues greater than the mean eigenvalues of PC axes generated by randomizing the morphological data across the tree 500 times (similar to "parallel analysis," Horn 1965). We further confirmed that PC axes were not correlated with body size using Spearman correlation analyses of PCA scores against the original body size values (PC1: $r^2 = -0.16$, r^2 adjusted $= 0.02$, $P = 0.07$; PC2: $r^2 = 0.11$, r^2 adjusted $= 0.01$, $P = 0.2$).

We examined whether each critical PC axis and body size evolved under a Brownian motion (BM) model (a random walk in which trait variance increases linearly through time with a motion rate parameter σ^2; Freckleton and Harvey 2006); or an Ornstein–Uhlenbeck (OU) model (incorporating both the rate parameter and a selective constraint towards an optimum value (α) to simulate evolution around an adaptive peak; Hansen and Martin, 1996; Hansen 1997; Butler and King 2004). The models were contrasted using ΔAIC and the maximum likelihood function "fitContinuous" (R package "geiger"; Harmon et al. 2008) for Cichlinae and each tribe independently. For all subsequent analyses, when an OU model was preferred over a BM model, each of the 1000 chronograms was transformed using the function ouTree (R package "geiger"; Harmon et al. 2008) and the value of α from the maximum likelihood model fitting prior to the calculation of independent contrasts or the simulation of morphological evolution.

ECOLOGICAL OPPORTUNITY AND RATES OF MORPHOLOGICAL EVOLUTION

We used maximum likelihood model-fitting analyses to examine whether rates of morphological evolution remained constant or changed over the evolutionary history of Neotropical cichlids (Mahler et al. 2010). We used the expected variance of standardized independent contrasts,

$$\sigma^2 = \frac{1}{n-1} \sum_{i=1}^{n-1} c_i^2 \tag{1}$$

calculated using the "pic" function in the R package "ape" (Felsenstein 1985; Paradis et al. 2004) to estimate a single, constant rate of morphological evolution (Revell 2008; Revell et al. 2007). Independent contrasts (based on OU transformed trees where necessary) were used as estimates of the Brownian motion parameter for the rate of morphological evolution for the branches over which they are calculated (McPeek 1995; Revell 2008). Following Mahler et al. (2010), we maximized for the summed log likelihood across all contrasts based on a single, constant rate of morphological evolution.

$$\log L(\sigma^2) = \sum_{i=1}^{n-1} \left[-\frac{1}{2} \left(\frac{c_i^2}{\sigma^2} + \ln(\sigma^2) + \ln(2\pi) \right) \right] \tag{2}$$

The model in eq. (2) was modified to account for changes in rates of morphological evolution through the evolutionary history of Neotropical cichlids. First, we examined whether the rate of morphological evolution changed through time using,

$$\log L(\sigma_0^2, \psi) = \sum_{i=1}^{n-1} \left[-\frac{1}{2} \left(\frac{c_i^2}{\psi^* t_i + \sigma_0^2} + \ln(\psi^* t_i + \sigma_0^2) + \ln(2\pi) \right) \right], \tag{3}$$

where t_i represents the relative age of the node across which contrasts were calculated (with the root at $t = 0$), σ_0^2 indicates rate of morphological evolution when $t = 0$, and ψ represents the slope of a regression of rate on time. Negative values of ψ indicate that rates of morphological evolution decreased through time, whereas positive values indicate a rate increase. We additionally examined whether the rate of morphological evolution changed with lineage diversity, by replacing t_i in eq. (3) with d_i, representing the number of lineages present in the tree at the age of each node relative to total lineage diversity. If rates of morphological evolution are dependent upon diversity, morphological evolution may have been influenced by competition between species (Mahler et al. 2010).

When a single model was not well supported over all others, we considered support for all models in which rates of morphological evolution changed through time by examining cumulative

Akaike weights for both time- and diversity-dependent models. Likelihood models described earlier were fitted for body size and critical PC axes across all sets of 1000 chronograms for the four focal clades using a modified version of the "fitDiversityModel" function from the "phytools" R Package (Revell 2012).

PATTERNS OF MORPHOLOGICAL EVOLUTION

We used "subclade disparity-through-time" (DTT) to examine patterns of morphological evolution of Neotropical cichlids (Harmon et al. 2003). These analyses compare the average disparity of all subclades to the overall disparity of a clade. Lower than expected values of average relative subclade disparity indicate that most morphological disparity originated early in the history of the group, whereas higher than expected values indicate that most morphological disparity originated more recently compared to a random walk pattern (Harmon et al. 2003). According to previous model fitting results, character evolution under a BM or OU model was simulated 1000 times for each tree in the posterior distribution as well as the MCC tree. The morphological disparity index (MDI) was calculated as the area between the observed DTT curve and the median DTT values from the simulated character histories. We calculated the difference between the observed MDI value and the MDI value of each of 1000 simulations for the lower two thirds of each tree (Slater et al. 2010; Derryberry et al. 2011) as a way to account for possible biases introduced by incomplete sampling of tip diversity. If the MDI values resulted from a constant rate model of evolution (either BM or OU) then, on average, the observed MDI values should be greater or less than the simulated values 50% of the time (respectively). For each tree, we determined frequency of simulated character histories that produced more extreme MDI values (> MDI_{obs} if MDI_{obs} is positive or < MDI_{obs} if MDI_{obs} is negative) than those observed (Slater et al. 2010; Derryberry et al. 2011). These steps were performed using the function "dtt.full" and mean-squared Euclidean distance as disparity (Foote 1997; Harmon et al. 2003) in the R package "geiger" (Harmon et al. 2008). We used this procedure for all critical PC axes and maximum body size in Cichlinae, Geophagini, Heroini, and Cichlasomatini separately.

Results

DIVERGENCE TIMES OF NEOTROPICAL CICHLIDS

We estimated a mean age of 150 Ma for the Cichlidae (95% HPD = 128.2–174.78, Node 161, Fig. 1, Appendix S2). The most recent common ancestor of the African and Neotropical clades was estimated at 147 Ma (124.49–171.05 Ma, Fig. 1, Node 160, Appendix 2). Divergence of Geophagini was estimated to start

at approximately 107 Ma (88.5–125.6 Ma, Node 109, Fig. 1). Separation of the tribes Cichlasomatini and Heroini was estimated at 95.4 Ma (76.7–114.7 Ma, Fig. 1). Differentiation of the crown group within each of these clades was estimated to start 81.7 Ma (64.8–99.9 Ma, Node 2, Fig. 1) for Cichlasomatini and 76.6 Ma (59.8–93.2 Ma, Node 3, Fig. 1) for Heroini. Separation of the basal branch leading to the Central American Heroini subclades was estimated at 54.2 Ma (42.7–65.6 Ma, Node 43, Fig. 1), with the origin of the two main Central American clades following at 50.2 (39.3–61.1 Ma) and 49.3 Ma (38.6–60.3 Ma), respectively.

PATTERNS OF LINEAGE DIVERSIFICATION

Lineage-through-time plots of Neotropical cichlids revealed clade-specific patterns (Fig. 2, with interpretation of only the lower two thirds of a clade's history). The LTT plot for Cichlinae and the tribe Geophagini revealed a decline in rate of lineage diversification toward the present, in both cases with a significant γ_{MCC} value (Fig. 2). When γ analyses were performed on the set of 1000 chronograms for each clade (not shown), only Geophagini γ values remained significant (mean $\gamma_{1000} = -1.95$, $P = 0.04$). Cichlasomatini LTT plots showed an initial increase followed by a sharp decline in lineage diversification at approximately 30 Ma, with a possible second period of diversification following the first increase; γ_{MCC} values for Cichlasomatini were not significant. Heroini LTT plots showed either a moderate initial increase or an approximately linear accumulation of diversity followed by a sharp decline ($\sim$60–50 Ma) and a relatively sudden increase in diversification apparently coincident with the origins of the Central American clades ($\sim$50–30 Ma). The slightly negative value of γ_{MCC} for Heroini was not significant. Except for Heroini, LTT plots showed decreasing lineage accumulation over time in all clades, but the γ statistic supported this trend only in Cichlinae and Geophagini.

Combined Akaike weights of all rate-variable models for Cichlinae, Geophagini, and Cichlasomatini were higher than 0.70, and in most cases exceeded 0.80, indicating that lineage diversification in these clades is unlikely to have followed constant-rate models (Table 2). The preferred variable-rate model was diversity dependent in all clades, but a multiple rate model (Yule-2-Rate) could not be confidently discarded (Table 2). In Heroini, the preferred model was a pure birth single rate model, but ΔAIC values were never high enough to discard variable rate models. In all cases, variable models supported a decline in rates of lineage accumulation (including Yule-2-Rate models).

PATTERNS OF PHENOTYPIC DIVERSIFICATION

Analysis of eight size- and phylogeny-corrected morphometric variables resulted in two critical principal components corresponding with two major axes of phenotypic variation (Table 3, Fig. 3). PC1 defined a gradient of variation between
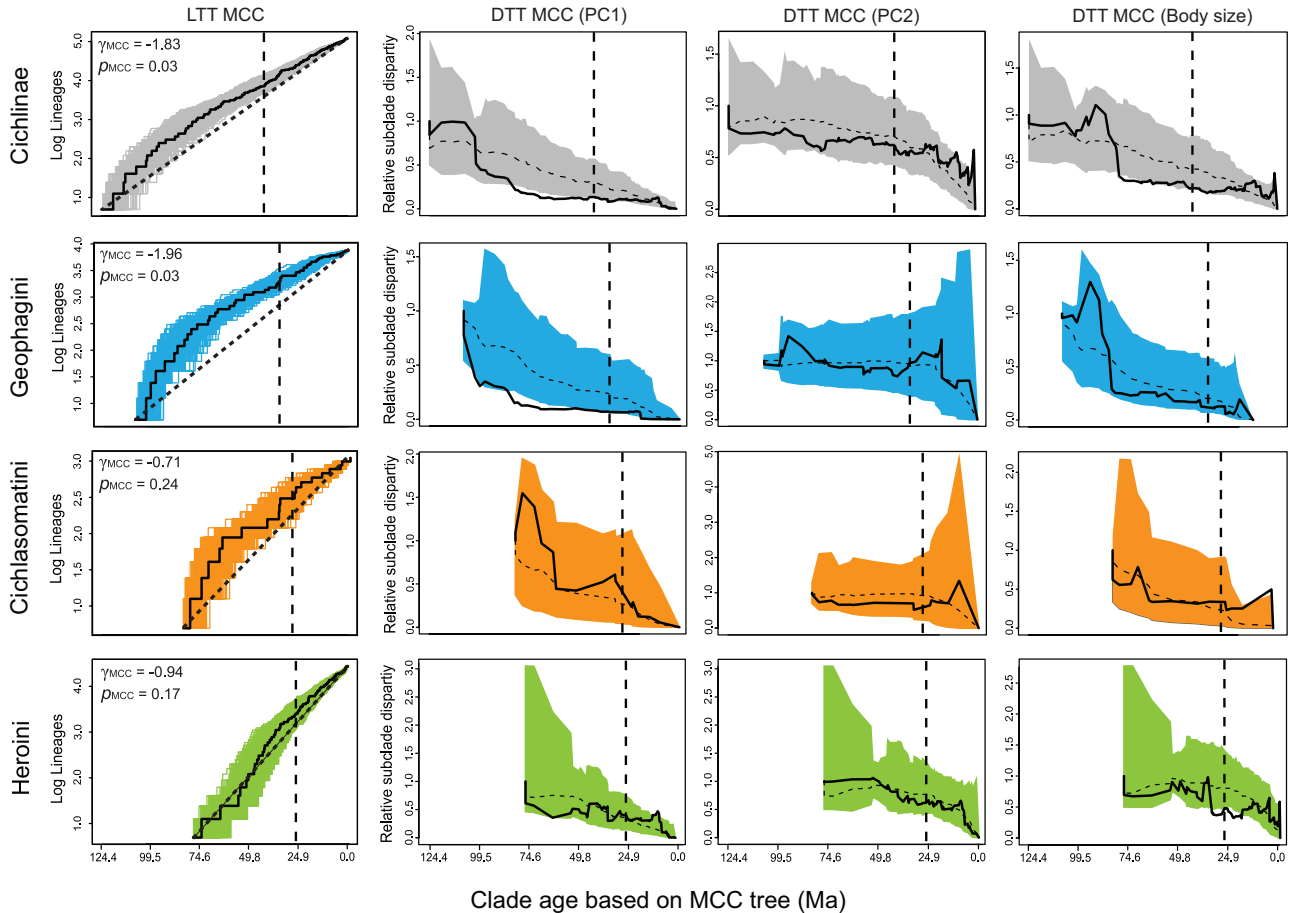
Figure 2. Patterns of lineage and subclade phenotypic disparity through time. Graphs are color-coded following the clade-specific colors from Figure 1. All model fitting analyses were based on chronograms from which the last third was truncated to minimize biases associated with incomplete taxon sampling of extant diversity; the point of truncation is indicated by vertical dashed lines and all interpretations in the text exclude the most recent third of the tree. The line is provided as a means to illustrate the portion of a clade's history that was analyzed in this article. LTT plots (left column) represent the MCC chronogram (black line) and 1000 chronograms sampled randomly from the posterior distribution of the Markov Chain Monte Carlo (MCMC) search during relaxed-clock dating in BEAST; the dashed line depicts the trajectory of a linear increase in diversity. Disparity through time plots (second from left to right-most columns) depict the 95% credibility interval for 1000 simulations of phenotypic disparity among subclades (shaded) and the median of the same simulation (dashed line) under either Brownian Motion (BM) or Ornstein–Uhlenbeck (OU) models as per model fitting results in Table 4. The black continuous line shows the actual pattern of subclade phenotypic disparity for the MCC tree. See Table 6 and the results section for summary analyses of subclade disparity for the 1000 random chronograms sampled along with the MCC tree. Analyses are based on chronograms standardized to a total length of 1 with time axis based on the MCC chronogram superimposed as a reference.

Table 3. Eigenvectors, eigenvalues, and variance explained by the first and second phylogenetic principal components analysis of phylogenetically size-corrected morphometric variables on the Bayesian MCC tree for Neotropical cichlids. PC1 summarizes variables broadly related to body shape and PC2 summarizes variables mostly related to trophic diversity associated with head shape.

Trait	Eigenvalue	% Variation Explained	Head Length	Head Height	Snout Length	Gape Width	Body Depth	Caudal Peduncle Depth	Eye Position	Eye Diameter
PC1	3.94	49.25	−0.26	−0.45	−0.32	−0.25	−0.43	−0.35	−0.44	−0.25
PC2	1.45	18.16	−0.62	0.12	−0.56	0.11	0.30	0.23	−0.09	0.35
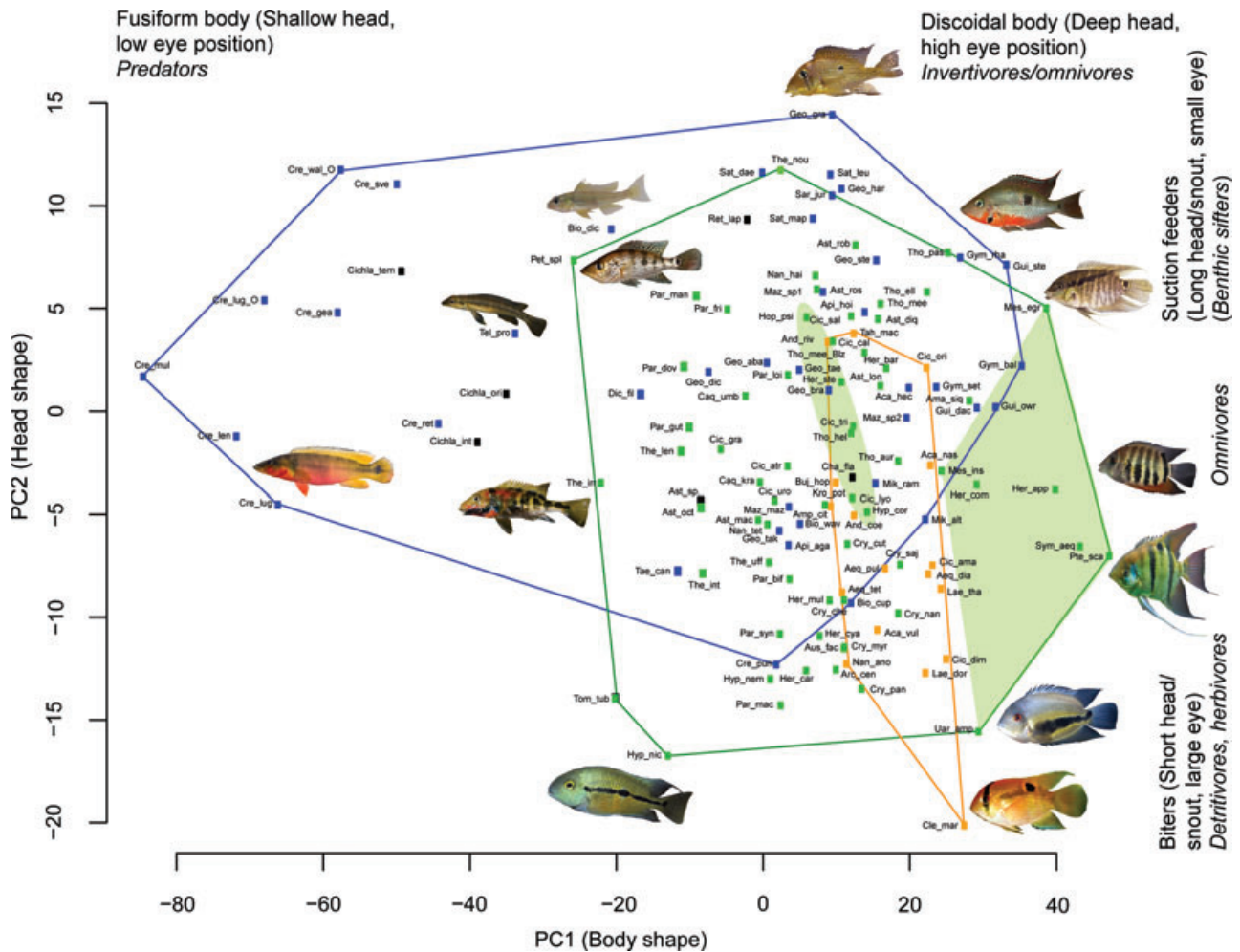
Figure 3. Phylogeny and size-corrected principal components analysis of eight morphometric variables for 575 individuals in 127 species of Neotropical cichlids. Polygons represent total morphospace for each of the three main tribes of Cichlinae using the same color codes as in Figure 1. Green-shaded areas represent morphospace occupied by South American Heroini. Photographs are intended to illustrate the morphology of taxa placed toward the extremes of morphological space. See text for explanation of variables and their ecomorphological interpretation. Photographs by H. López-Fernández and courtesy of K. M. Alofs and A. Lamboj.

fishes with fusiform bodies (i.e., shallow bodies, heads, and caudal peduncles) and eyes positioned dorsally (*Crenicichla lugubris*, *Petenia splendida*; Table 3, Fig. 3) and fishes with a relatively discoid body shape (i.e., deep bodies and heads) and eyes positioned medially (*Guianacara*, *Pterophyllum*; Table 3, Fig. 3). The positive extreme of PC2 represented fishes with long heads and snouts and small eyes (e.g., *Geophagus grammepareius*, *Astatheros robertsoni*; Table 3, Fig. 3), and the negative extreme represented fishes with short heads and snouts and larger eyes (e.g., *Cleithracara maronii*, *Hyposphrys nicaraguense*; Table 3, Fig. 3). We refer to these axes as defining principal gradients of body shape variation (PC1) and head shape variation (PC2). The basal Neotropical genus *Cichla* and especially the geophagine clade including *Crenicichla* and *Teleocichla* occupy a unique region of morphospace at the negative extreme of PC1, characterized by extremely elongate and shallow bodies (Table 3, Fig. 3, blue poly-

gon). The Heroini species *Petenia splendida* and *Theraps irregularis* are the only non-geophagine taxa approaching this fusiform morphology. Toward the positive end of PC1, some South American heroine taxa have evolved extreme discoid body shapes that no other clade shares (e.g., *Pterophyllum*, *Symphysodon*, Fig. 3, green polygon). Variation in head morphology (PC2) is less conspicuous, but nonetheless taxa within the Heroini and some Cichlasomatini have diverged into a region of morphospace with short heads and snouts not shared by any lineage of Geophagini (Fig. 3, green and orange polygons). The Geophagini clearly occupies the largest volume of morphospace, followed by the Heroini. These two clades have areas of overlap in morphological space involving species of South American heroines and geophagines. The Cichlasomatini occupies a comparatively restricted portion of total morphospace that overlaps the other clades, and only one of its taxa appears to have diverged into a morphology not shared

Table 4. Maximum likelihood model fitting results comparing a model of Brownian Motion (BM) evolution to an Ornstein–Uhlenbeck (OU) evolution. Values are summarized across 1000 chronograms randomly sampled from the posterior distribution of the BEAST MCMC analysis.

	Log L_{BM}	Log L_{OU}	ΔAIC_{BM}	ΔAIC_{OU}	w_{BM}	w_{OU}	α_{OU}	Model
Cichlinae								
PC1	−508	−508	0.03	2.03	0.729	0.271	2.42E-04	BM
PC2	−443	−427	30.5	0.06	0.025	0.975	1.35	OU
Body size	−113	−104	15.6	0.00	0.003	0.997	1.48E-02	OU
Geophagini								
PC1	−170	−170	0.00	2.34	0.763	0.237	4.01E-05	BM
PC2	−148	−134	24.5	0.11	0.046	0.954	4.69	OU
Body size	−30.9	−30.9	0.00	2.31	0.760	0.240	1.19E-04	BM
Cichlasomatini								
PC1	−53.5	−53.1	0.00	2.21	0.748	0.252	1.38E-02	BM
PC2	−58.4	−53.3	7.18	0.09	0.091	0.909	11.6	OU
Body size	−6.42	−5.42	0.22	1.39	0.634	0.366	2.28	BM
Heroini								
PC1	−247	−246	0.66	0.79	0.545	0.455	1.03E-02	BM
PC2	−213	−206	11.7	0.02	0.022	0.978	5.10E-02	OU
Body size	−56.0	−43.3	23.2	0.00	0.000	1.000	2.25	OU

by other lineages (*Cleithracara maronii*, Fig. 3, orange polygon). Model fitting of PCA scores revealed that body shape evolution (PC 1) was better described under a BM model for all clades, whereas head shape (PC2) fit an OU model in all cases (Table 4). Body size variation fit an OU model for Cichlinae and Heroini, but Geophagini and Cichlasomatini followed a BM model of body size divergence (Table 4).

A constant rate model was marginally preferred to describe rates of morphological diversification for PC1 (body shape) in Cichlinae, and either constant rate or diversity-dependent diversification models were more likely for PC2 (head shape) and body size variation (Table 5). Although not supported by model fitting (Table 5) or the MDI values (22.0%, Table 6), a deceleration in morphological diversification of PC1 attributes is suggested by the negative departure of the observed DTT curve from BM expectations (Fig. 2) between ∼100 and ∼50 Ma. Constant rate under an OU model of evolution in PC2 (head shape) could not be discarded based on model fitting (Table 5), DTT plots or MDI values, suggesting that variation of head shape has accumulated adaptively during the clade's history. Although not supported by model fitting, a decrease in rate or relaxation of selection on body size divergence across Cichlinae starting about ∼75 Ma is strongly suggested by the DTT plots (Fig. 2) and the negative MDI values with low frequency of more extreme values observed for the group (Table 6).

Body shape (PC1) within Geophagini revealed moderate support for decreased rates of morphological evolution ($\Delta AIC_{constant} = 2.42$, cumulative wAIC = 0.78 for time and diversity-dependent models, $\psi = -0.06$ and -0.15 respectively;

Table 5). This pattern is supported by an extremely low DTT curve (Fig. 2) and a negative MDI value exceeded only by about 2% of all MDI simulations, strongly indicating an early burst in body shape diversification. Geophagini head shape (PC2) and body size weakly fit constant-rate models of diversification (Table 5), a trend supported by the DTT plots (Fig. 2) and average MDI values close to the expectation of 0 (Table 6). Unlike body size, however, head shape evolution fit an OU model (Table 4), suggesting that diversification of head attributes has remained constrained by selection.

Morphological diversification in Cichlasomatini fit a constant-rate model for PC1 and body size. No single model was strongly supported for PC2 (Table 5), which may result from the small number of contrasts possible for the model fitting analyses given the relatively small number of lineages in the clade. Nevertheless, PC2 evolution followed an OU model (Table 4), suggesting that the constant rate of morphological diversification may be driven by adaptive constraints on head shape variation.

In Heroini, there was no strong support for one model of rates of morphological evolution along PC1, and a constant-rate model could not be discarded for PC2. But divergence in PC2 followed an OU model (Table 4), suggesting linear accumulation of adaptive change in head shape attributes. Body size diversification fit a constant rate model of evolution under an OU model (Tables 4 and 5), but a mild time-dependent deceleration in body size divergence could not be discarded (Table 5). The DTT analysis showed a negative MDI value exceeded only by less than 9% of MDI simulations (Fig. 2). Because OU models incorporate both a selection parameter (α) and a rate parameter (σ), the

Table 5. Comparison of models of phenotypic diversification. Standard error incorporates both estimation error and phylogenetic uncertainty.

Clade	Trait	Model	σ_0^2(SE)	ψ(SE)	log(L)	ΔAIC	wAIC
Cichlinae	PC1	Constant rate	4.05 (1.13)	–	−508.6	0.10	0.53
		Diversity	3.69 (0.99)	5.36×10^{-3} (1.41×10^{-2})	−508.3	1.59	0.25
		Time	4.19 (1.56)	-1.67×10^{-3} (1.79×10^{-2})	−508.4	1.83	0.22
	PC2	Constant rate	1.46 (0.78)	–	−428.0	1.77	0.44
		Diversity	1.32 (1.42)	1.67×10^{-3} (1.34×10^{-2})	−427.0	1.84	0.31
		Time	1.46 (1.80)	1.41×10^{-4} (1.77×10^{-3})	−427.2	2.34	0.25
	Body size	Constant rate	7.97×10^{-3} (2.22×10^{-3})	–	−104.4	0.00	0.53
		Diversity	6.54×10^{-3} (5.45×10^{-3})	1.47×10^{-5} (4.32×10^{-5})	−104.0	1.34	0.27
		Time	7.85×10^{-3} (7.53×10^{-3})	1.22×10^{-6} (7.11×10^{-5})	−104.4	2.04	0.19
Geophagini	PC1	Constant rate	4.31 (2.86)	–	−170.1	2.42	0.22
		Diversity	7.466 (2.85)	-0.149 (3.28×10^{-2})	−168.0	0.52	0.39
		Time	8.00 (3.36)	-6.19×10^{-2} (1.65×10^{-2})	−168.0	0.47	0.39
	PC2	Constant rate	1.48 (1.13)	–	−135.8	0.29	0.50
		Diversity	2.39 (1.87)	-2.66×10^{-2} (5.24×10^{-2})	−135.3	1.52	0.26
		Time	2.38 (1.92)	-9.59×10^{-3} (1.91×10^{-2})	−135.4	1.64	0.24
	Body size	Constant rate	4.23×10^{-3} (2.25×10^{-3})	–	−30.9	0.01	0.53
		Diversity	5.25×10^{-3} (2.12×10^{-3})	-4.61×10^{-5} (7.54×10^{-5})	−30.6	1.62	0.24
		Time	5.51×10^{-3} (2.38×10^{-3})	-2.16×10^{-5} (3.62×10^{-5})	−30.6	1.64	0.23
Cichlasomatini	PC1	Constant rate	0.693 (0.931)	–	−53.5	0.00	0.62
		Diversity	0.579 (0.791)	1.39×10^{-2} (8.01×10^{-2})	−53.4	2.40	0.19
		Time	0.573 (0.830)	2.86×10^{-3} (1.63×10^{-2})	−53.4	2.42	0.19
	PC2	Constant rate	1.18 (1.96)	–	−53.3	0.11	0.51
		Diversity	2.92 (2.45)	-0.130 (0.161)	−52.7	1.49	0.25
		Time	2.73 (2.30)	-2.30×10^{-2} (3.04×10^{-2})	−52.7	1.59	0.24
	Body size	Constant rate	2.87×10^{-3} (7.24×10^{-3})	–	−6.4	0.00	0.51
		Diversity	1.77×10^{-3} (2.49×10^{-3})	1.24×10^{-4} (2.36×10^{-4})	−5.8	1.50	0.24
		Time	1.80×10^{-3} (2.17×10^{-3})	2.29×10^{-5} (3.89×10^{-5})	−5.8	1.45	0.25
Heroini	PC1	Constant rate	4.62 (2.88)	–	−247.5	0.84	0.33
		Diversity	2.97 (1.60)	4.65×10^{-2} (4.13×10^{-2})	−246.1	0.20	0.44
		Time	2.80 (2.01)	0.0345 (0.0370)	−246.7	1.43	0.23
	PC2	Constant rate	1.56 (2.27)	–	−205.5	0.15	0.52
		Diversity	1.27 (2.38)	7.51×10^{-3} (8.29×10^{-3})	−205.2	1.73	0.23
		Time	1.06 (1.40)	8.84×10^{-3} (2.66×10^{-2})	−205.1	1.56	0.25
	Body size	Constant rate	1.11×10^{-3} (1.73×10^{-3})	–	−43.3	0.00	0.56
		Diversity	1.23×10^{-3} (1.85×10^{-3})	-2.12×10^{-5} (2.77×10^{-4})	−43.3	2.02	0.21
		Time	1.51×10^{-3} (1.38×10^{-3})	-6.15×10^{-5} (1.90×10^{-4})	−43.2	1.81	0.23

negative MDI may be indicative of either a relaxation of selection or deceleration in the rate of body size divergence. These findings suggest that Heroini may have undergone adaptive body size diversification for part of their history. This trend toward deceleration or relaxed selective constraints appears associated with a sharp decrease in body size subclade disparity initiated some ∼30 Ma as indicated in the DTT plot (Fig. 2).

Discussion
THE AGE OF CICHLIDS
Our estimates suggest a late Jurassic (∼150 Ma) age for the Cichlidae, and the 95% HPD intervals provide a range between the Middle Jurassic and the middle Lower Cretaceous (Fig. 1). This generally agrees with previous studies suggesting a Cretaceous age for cichlids (Genner et al. 2007; Azuma et al. 2008), but contrasts with others that placed their origin in the Paleogene (e.g., Santini et al. 2009). Genner et al. (2007) estimated an age between 122.5 and 151.8 Ma from calibrations using Gondwanan fragmentation; however, their fossil-based calibration revealed a considerably younger age (45.7–46.3 Ma). This discrepancy derives from imposing hard upper and lower bounds to calibrate the root node of cichlids with the African fossil †*Mahegenchromis* (45.7–46.3 Ma, Murray 2000). Given that fossils provide minimum but not maximum estimates of clade age (Lundberg 1993; Parham et al.

Table 6. Results of the disparity-through-time (DTT) analyses (all results summarized across all 1000 chronograms) with the last third of the chronogram truncated to account for incomplete taxonomic sampling. Character evolution was simulated either under a Brownian Motion (BM) or Ornstein–Uhlenbeck (OU) model of evolution based on maximum likelihood model fitting analyses (see Table 4). Mean observed morphological disparity index (MDI, area between the observed curve and the median simulated DTT curve) ± standard deviation and the frequency of 1000 simulated DTT curves that produced more extreme MDI values than the observed data are also given.

Clade	Trait	Model	MDI (Truncated)	Frequency of More Extreme Simulated MDI Values (Truncated)
Cichlinae	PC1	BM	−0.059 ± 0.039	0.220
	PC2	OU	−0.072 ± 0.064	0.181
	Size	OU	−0.114 ± 0.027	0.071
Geophagini	PC1	BM	−0.178 ± 0.037	0.021
	PC2	OU	−0.035 ± 0.14	0.266
	Size	BM	0.012 ± 0.029	0.405
Cichlasomatini	PC1	BM	0.143 ± 0.058	0.239
	PC2	OU	−0.153 ± 0.072	0.166
	Size	BM	−0.003 ± 0.026	0.439
Heroini	PC1	BM	−0.081 ± 0.067	0.161
	PC2	OU	0.028 ± 0.074	0.373
	Size	OU	−0.111 ± 0.036	0.089

2012), use of this fossil to make a rigid maximum bound for the root node age is a severe constraint. The incompatibility of Genner et al.'s (2007) two estimates is a result of the constraint employed rather than a conflict between fossil and biogeographic calibration dates. In a more general sense, using †*Mahengechromis* as a minimum-age estimate of the entire family may also bias the results by assuming the fossil is close to the root. This assumption is questionable given the inconclusive phylogenetic placement of the fossil (Murray 2001; Sparks 2004). This consideration may also affect estimates from another recent study. Santini et al. (2009) used extensive sampling of teleost RAG1 sequences, including 8 cichlid lineages and 45 fossil calibrations, two of which were cichlids, to provide a time-line of actinopterygian divergence, yielding an age for Cichlidae of 46–73 Ma. They used †*Mahengechromis* as a minimum age estimate for the root node of cichlids, and the minimum age of a fossil otolith (84 Ma) attributable to Perciformes as the upper bound for the maximum age of cichlids (Santini et al. 2009, Supplementary Materials). Unfortunately, although this fossil provides a minimum age estimate for Perciformes (which presumably includes cichlids, but see Near et al. 2012; Wainwright et al. 2012), by definition it does not inform the maximum age of either Perciformes or cichlids, artificially constraining the age of cichlids to be younger than 84 Ma. Azuma et al. (2008) obtained estimates of cichlid ages that are compatible with Gondwanan fragmentation patterns based on an extensive set of 21 external fossil calibrations and mitogenomic sequences.

Our study also has assumptions with the potential to bias the age estimate for the Cichlidae toward greater values than those obtained by several previous studies. Chief among them is the root height prior used to constrain the maximum age of the family. We used the 121 to 165 Ma estimate for the separation of eastern and western Gondwana (see Appendix S1 and Genner et al. 2007) reflecting the plausible scenario that the main cichlid lineages originated through vicariance during Gondwanan fragmentation. Although our approach does not provide an independent test of the Gondwanan-divergence hypothesis, it is based on our current understanding of phylogenetic relationships among major lineages of Cichlidae. An additional source of incongruence between our estimates and those based on purely nuclear sequences could be associated with differences in rates of molecular evolution (e.g., Lukoschek et al 2012; Near et al. 2012). Future research on the origin of Cichlidae should provide additional insight on the effects of the many factors that may be affecting current age estimates, including those presented in this article.

ECOMORPHOLOGICAL DIFFERENTIATION AND CONVERGENCE WITHIN AND AMONG CLADES

Morphological and trophic diversification patterns among and within the main clades of Neotropical cichlids were consistent with findings from earlier studies of ecomorphology and functional morphology in the group (Winemiller et al. 1995; Hulsey and García de León 2005; López-Fernández et al. 2012). Morphometric results from our PC analyses are consistent with feeding performance results from Wainwright et al. (2001), suggesting that PC1 represents a gradient of ram-suction feeding with large-gaped piscivores placed towards the ram end of the gradient (negative PC1, Fig. 3) and suction feeders dominating the positive end of the gradient (Fig. 3, López-Fernández et al. 2012). Variation along PC1 probably represents more than just trophic divergence along a ram-suction feeding gradient, because body shape also influences swimming performance, which in turn is directly related to habitat use (e.g., Webb 1982; Webb et al. 1996).

Variation along PC2 is associated with different modes of prey capture. Unlike body shape divergence, the fit to a constant-rate OU model indicates that head shape diversification in all Neotropical cichlids occurred continuously and under strong selective constraints. Deeper-bodied fishes along PC2 varied in snout and head length, which are related to mouth protrusion (López-Fernández et al. 2012). Fish with long snouts along the positive end of PC2 were specialized substrate sifters (e.g., *Geophagus*), whereas fish with shorter snouts toward the negative end of PC2 tended to be strong biters (e.g., *Tomocichla*) feeding on detritus, algae turfs, or fruit (Winemiller et al. 1995; Hulsey and García de León 2005; López-Fernández et al. 2012). Variation in eye diameter along PC2 could reflect the role of vision in prey

capture. Winemiller et al. (1995) found a negative correlation between piscivory and relative eye size, and Goatley and Bellwood (2010) discussed the role of visual acuity (linked to eye size) in the ability of fish to consume specific types of prey.

The widespread morphological convergence among Neotropical cichlid lineages is perhaps even more interesting than examples of uniquely divergent forms. Several predatory lineages evolved toward an elongate body and ram-feeding form with its most extreme example in the geophagine *Crenicichla*. This convergent morphology evolved independently in the basal genus *Cichla* and the heroine genera *Petenia* and *Parachromis*, all of which are piscivores (Winemiller et al. 1995, 1997; Cochran-Biederman and Winemiller 2010). Interestingly, some non-piscivorous taxa within Geophagini (e.g., *Dicrossus*), Retroculini (*Retroculus*), and Heroini (e.g., *Tomocichla*) also have elongate bodies. In these lineages, however, this body shape seems more likely to be associated either with fast water current (e.g., *Retroculus*, *Teleocichla*, some *Theraps*, Zuanon 1999; Soria-Barreto and Rodiles-Hernández 2008) or with structurally complex habitats (*Biotoecus*, Willis et al. 2005). A strong association between morphology and diet also is evident among species grouped at the positive end of PC2. Many benthivorous geophagines (*Geophagus*, *Satanoperca*, *Guianacara*), heroines (*Thorichthys*, *Astatheros*), and retroculines (*Retroculus*) overlapped in this region of morphospace, indicating similarity in body and head shape attributes. Although this space is not entirely restricted to substrate-sifting taxa (e.g., *Nandopsis*, a predator, Fig. 3), these results reveal convergence in traits of specialized benthic-feeding fishes.

Divergence in body shape (PC1) is consistent with a BM model (Table 4) in which lineages appear to have exploited new regions of morphospace, particularly during early divergence of Geophagini, which is the only clade that shows an early burst of morphological diversification (Fig. 2). Extensive convergence along PC1 is not observed until the Eocene expansion of heroines into Central America, but unlike geophagines, heroines show no evidence of an accelerated rate of body shape divergence (Fig. 2). Contrastingly, adaptive divergence along PC2 under an OU model may be at least partly responsible for the extensive convergence in head shape and trophic specialization among different Neotropical cichlid clades, particularly geophagines, cichlasomatines, and Central American heroines (Fig. 2). It is possible that feeding mechanics, which underlies much of head shape variation, imposes restrictions on morphological diversification (Hulsey & Wainwright 2002), keeping head shape variation under strong selective pressure by the demands of feeding performance.

TIMING OF PHENOTYPIC DIFFERENTIATION AND CLADE-SPECIFIC PATTERNS OF DIVERSIFICATION

Divergence patterns in Cichlinae revealed a significant deceleration in lineage accumulation, accompanied by lower than expected

relative subclade disparity in body shape and body size divergence during at least some periods of the group's history (Fig. 2, Table 6). This clade-wide pattern, however, is derived from the combination of lineage-specific paths of diversification. Although their ancestral lineages were contemporaries, Geophagini underwent phyletic and ecomorphological diversification much earlier than Heroini and Cichlasomatini. As depicted in the LTT plot (Fig. 2), the rate of lineage accumulation in Geophagini started decelerating fairly early in the clade's history, and it may have done so in a diversity-dependent manner (Table 2). This pattern corresponds with the sudden decline in rate of body shape (PC1) differentiation after the two main subclades of Geophagini diverged from each other (Figs. 1 and 2, Tables 5 and 6), probably marked by the appearance of piscivory within the *Crenicichla* clade. It was not until morphological differentiation in Geophagini was well underway that the crown lineages of Cichlasomatini and Heroini started diverging. Cichlasomatine taxa tend to be ecological generalists (Winemiller et al. 1995) and revealed the least head shape differentiation (Table 4, $\alpha = 11.6$). Early diversification of geophagines could have produced superior competitors that constrained cichlasomatine niche diversification in areas of sympatry. In modern local fish assemblages of lowland rivers within the Orinoco and Amazon basins, cichlasomatines tend to be poorly represented when compared to geophagines (Kullander 1986; Winemiller et al. 2008; Montaña and Winemiller 2010). Cichlasomatines tend to be more abundant in Andean piedmont streams where geophagine diversity is lower, and on the Pacific slope of the Andes where geophagines are rare or absent.

The novel regions of body shape morphospace occupied by Heroini and Geophagini in South America probably illustrate the role of ecological opportunity and competitive exclusion in shaping the evolution of ecomorphological diversity in Neotropical cichlids. Geophagine diversification involved considerable morphological innovation (e.g., *Crenicichla*, Fig. 3), and presumably affected heroine diversification by driving the evolution of ecomorphological extremes in the South American lineages of Heroini. With the exception of *Hoplarchus* (a monotypic genus) and *Hypselecara* (two species), morphospace of the endemic South American heroines does not overlap with that of geophagines (Fig. 3, green-shaded areas). Heroine invasion of Central America, where geophagines are absent, allowed this clade to diversify into wider ecomorphological space than it occupies in South America; but body shape diversification in Central American heroines did not follow a pattern of explosive diversification as that observed among South American geophagines. Taken together, the timing of clade diversification, observed patterns of morphological divergence, and a potential rate shift or relaxed selection pressure in body size evolution suggest that colonization of Central America provided Heroini with opportunities for novel ecomorphological diversification.

ANCIENT ADAPTIVE RADIATION OR A LONG HISTORY OF GRADUAL ADAPTIVE DIVERSIFICATION?

Molecular phylogenetic analyses of geophagine cichlids and of all Cichlinae led to the idea that Geophagini, Heroini, and perhaps Cichlasomatini may have diversified through adaptive radiation (López-Fernández et al. 2005, 2010). Slowing rates of Cichlinae diversification appear to be influenced by a strong pattern of deceleration in lineage accumulation within Geophagini, as evidenced by the γ-statistic, LTT plots, and likelihood models fitted with single and variable rates of lineage diversification. Model-fitting analyses also supported declining rates of lineage diversification over time in Cichlasomatini. Thus, with the exception of Heroini, our lineage analyses are compatible with an early-burst model of diversification within two of the main subclades of Cichlinae, followed by lower rates of diversification (overshooting). Both of these patterns are typically associated with adaptive radiation (Gavrilets and Losos 2009).

Trends in phenotypic divergence are more complex and much more variable among clades and sets of morphological attributes. In Geophagini, phenotypic differentiation along PC1 is congruent with what could be viewed as an "ancient adaptive radiation." Declining body shape disparity within subclades (Fig. 2, Table 5) began even as lineage diversification was still at its maximum rate of increase. Early morphological divergence followed by significant deceleration along PC1 is congruent with expectations during an adaptive radiation (Harmon et al. 2003; Gavrilets and Losos 2009). Geophagini show another attribute of adaptive radiations, namely evidence for "least action effect," or minimal phenotypic change after the initial burst of diversification (Gavrilets and Losos 2009). Deceleration in the evolution of geophagine body shape is a finding congruent with the remarkable morphological stasis demonstrated by Eocene fossils attributable to modern taxa such as †*Gymnogeophagus eocenicus* (Malabarba et al. 2010). Geophagini appear to have undergone an early and rapid diversification of body shape that was accompanied by continuous trophic diversification reflected in morphological divergence in head attributes.

Morphological divergence in Cichlasomatini and Heroini does not show patterns as distinct as those of Geophagini. Again, the South American Cichlasomatini and Heroini may have been prevented from undergoing adaptive radiation by the earlier radiation of Geophagini. Conceivably, recent phenotypic diversification within Central American Heroini represents the early stage of an adaptive radiation with overshooting not yet evident (see Hulsey et al. 2010). The great ecomorphological diversity of Central American Heroini is consistent with the idea of ecological release in the absence of geophagine competitors and suggests that heroine cichlids in Central America are undergoing further ecomorphological diversification. Support for this view comes from the relatively low subclade disparity in body size (Fig. 2) and the extensive ecomorphological convergence between Central American Heroini and South American Geophagini (Fig. 3).

Some models of adaptive radiation incorporated the concept of "radiation in stages" (Streelman and Danley 2003), in which divergence along different ecological axes occurs in a succession of diversification events: habitat first, diet second, communication third. This idea is based largely on the observation that habitat-related divergence often occurs near the base of a tree, with trophic-related divergence generally occurring within clades that already underwent habitat specialization. The pattern of morphological evolution within the geophagine radiation is consistent with these previous observations: (1) evolution in body shape, which affects habitat use, occurs as an early burst (PC1, Fig. 2); whereas (2) subclades with distinct body shapes continue to acquire trophic morphologies that ultimately result in high trophic diversity within body shape groups (PC2, Figs. 2 and 3). The mechanism behind this pattern, at least within Geophagini, appears to be driven by a difference in the constraints on evolution between morphological axes. Although divergence in body shape (PC1) represents exploration of new areas of morphospace under an unconstrained BM model, diversification in head shape (PC2) is constrained by functional morphological constraints on feeding performance. In other words, the appearance of "diversification in stages" emerges as a product of the differences in evolutionary constraints and opportunities between the two axes, rather than differences in their evolutionary tempos per se.

Neotropical cichlids diverged from African cichlids during or before the early Cretaceous. Major clades within Cichlinae evolved along divergent trajectories during different periods. In addition to selection imposed by environmental conditions during the Upper Cretaceous and Paleogene, ecological interactions among the diversifying lineages probably played an important role in these evolutionary trajectories, as inferred by the extensive diversification of heroines in Central America compared with members of the clade in South America where they coexist with geophagines. Patterns of lineage and phenotypic divergence indicate that Geophagini represents an ancient adaptive radiation. Our results also suggest that Central American heroines, a clade originated during the Eocene, may represent an ongoing adaptive radiation facilitated by the ecological opportunity provided by the absence of geophagines. Diversification in the South American Cichlasomatini may have been limited by the dominance of the older and more diverse geophagine lineages in lowland aquatic habitats. New methods for dating molecular phylogenies and for discerning modes of lineage and phenotypic divergence have allowed us to examine patterns of diversification over large scales of time and space for one of the most diverse families of fishes in the Neotropics.

LITERATURE CITED

Alano-Pérez, P., M. Malabarba, and C. Del Papa. 2010. A new genus and species of Heroini (Perciformes: Cichlidae) from the early Eocene of southern South America. Neotrop. Ichthyol. 8:631–642.

Azuma, Y., Y. Kumazawa, M. Miya, K. Mabuchi, and M. Nishida. 2008. Mitogenomic evaluation of the historical biogeography of cichlids toward reliable dating of teleostean divergences. BMC Evol. Biol. 8:215.

Baldwin, B. 1997. Adaptive radiation of the Hawaiian silversword alliance: congruence and conflict of phylogenetic evidence from molecular and non-molecular investigations. Pp. 103–128 in T. J. Givnish, and K. J. Sytsma, eds. Molecular evolution and adaptive radiation. Cambridge Univ. Press, Cambridge, U.K.

Burbrink, F. T., and R. A. Pyron. 2010. How does ecological opportunity influence rates of speciation, extinction, and morphological diversification in new world ratsnakes (Tribe Lampropeltini)? Evolution 64:934–943.

Burnham, K., and D. Anderson. 2002. Model selection and multimodel inference: a practical information-theoretic approach. Springer, New York, NY.

Butler, M. A., and King, A. A. (2004). Phylogenetic comparative analysis: a modeling approach for adaptive evolution. Am. Nat. 164:683–695.

Claramunt, S. 2010. Discovering exceptional diversifications at continental scales: the case of the endemic families of neotropical suboscine passerines. Evolution 64:2004–2019.

Claramunt, S., E. Derryberry, R. Brumfield, and J. Remsen. 2012. ecological opportunity and diversification in a continental radiation of birds: climbing adaptations and cladogenesis in the Furnariidae. Am. Nat. 179:649–666.

Cochran-Biederman, J., and K. Winemiller. 2010. Relationships among habitat, ecomorphology and diets of cichlids in the Bladen River, Belize. Environ. Biol. Fishes 88:143–152.

Derryberry, E., S. Claramunt, G. Derryberry, R. Chesser, J. Cracraft, A. Aleixo, J. Pérez-Emán, J. Remsen, and R. Brumfield. 2011. Lineage diversification and morphological evolution in a large-scale continental radiation: the neotropical ovenbirds and woodcreepers (aves: Furnariidae). Evolution 65:2973–2986.

Dornburg, A., J. M. Beaulieu, J. C. Oliver, and T. J. Near. 2012. Integrating fossil preservation biases in the selection of calibrations for molecular divergence time estimation. Syst. Biol. 60:519–527.

Drummond, A., S. Ho, M. Phillips, and A. Rambaut. 2006. Relaxed phylogenetics and dating with confidence. PLoS Biol. 4:e88.

Drummond, A. J., and A. Rambaut. 2007. BEAST: Bayesian evolutionary analysis by sampling trees. BMC Evol. Biol. 7:214.

Farias, I. P., G. Ortí, and A. Meyer. 2000. Total evidence: molecules, morphology, and the phylogenetics of cichlid fishes. J. Exp. Zool. 288:76–92.

Felsenstein, J. 1985. Phylogenies and the comparative method. Am. Nat. 125:1–15.

Foote, M. 1997. The evolution of morphological diversity. Ann. Rev. Ecol. Syst. 28:129–152.

Fordyce, J. 2010. Interpreting the gamma statistic in phylogenetic diversification rate studies: a rate decrease does not necessarily indicate an early burst. PLoS ONE 5:e11781.

Freckleton, R., and P. Harvey. 2006. Detecting non-Brownian trait evolution in adaptive radiations. PLoS Biol. 4:e737.

Froese, R., and D. Pauly. 2011. FishBase. Available at www.fishbase.org/search.php. Accessed 4 January 2012.

Gavrilets, S., and J. B. Losos. 2009. Adaptive radiation: contrasting theory with data. Science 323:732–737.

Genner, M., O. Seehausen, D. Lunt, D. Joyce, P. Shaw, G. Carvalho, and G. Turner. 2007. Age of cichlids: new dates for ancient lake fish radiations. Mol. Biol. Evol. 24:1269–1282.

Glor, R. 2010. Phylogenetic insights on adaptive radiation. Annu. Rev. Ecol. Evol. Syst. 41:251–270.

Goatley, C., and D. Bellwood. 2010. Fishes on coral reefs: changing roles over the past 240 million years. Paleobiology 36:415–427.

Grant, P., and B. Grant. 2008. How and why species multiply. Princeton Univ. Press, Princeton, NJ.

Hansen, T. F. 1997. Stabilizing selection and the comparative analysis of adaptation. Evolution 51:1341–1351.

Hansen, T. F., and Martins, E. P. 1996. Translating between microevolutionary process and macroevolutionary patterns: the correlation structure of interspecific data. Evolution 50:1404–1417.

Harmon, L. J., J. A. Schulte, A. Larson, and J. B. Losos. 2003. Tempo and mode of evolutionary radiation in iguanian lizards. Science 301:961–964.

Harmon, L. J., J. T. Weir, C. D. Brock, R. E. Glor, and W. Challenger. 2008. GEIGER: investigating evolutionary radiations. Bioinformatics 24:129–131.

Ho, S. Y. W. 2007. Calibrating molecular estimates of substitution rates and divergence times in birds. J. Avian. Biol. 38:409–414.

Horn, J. 1965. A rationale and test for the number of factors in factor analysis. Psychometrika. 32:179–185.

Hulsey, C. D., and P. C. Wainwright. 2002. Projecting mechanics into morphospace: disparity in the feeding system of labrid fishes. Proc. R. Soc. Lond. B 269:317–326.

Hulsey, C. D., and F. García de León. 2005. Cichlid jaw mechanics: linking morphology to feeding specialization. Funct. Ecol. 19:487–494.

Hulsey, C. D., P. R. Hollingsworth, and J. A. Fordyce. 2010. Temporal diversification of Central American cichlids. BMC Evol. Biol. 10:279.

Kocher, T. 2004. Adaptive evolution and explosive speciation: the cichlid fish model. Nat. Rev. Genet. 5:288–298.

Kornfield, I., and P. Smith. 2000. African cichlid fishes: Model systems for evolutionary biology. Ann. Rev. Ecol. Syst. 31:163–196.

Kullander, S. O. 1986. Cichlid fishes of the Amazon River drainage of Peru. Swedish Museum of Natural History, Stockholm.

———. 2003. Family Cichlidae (Cichlids). Pp. 605–656 in R. RE, S. O. Kullander, and C. J. Ferraris Jr, eds. Check list of the freshwater fishes of South and Central America. Museu de Ciências e Tecnologia – Pontifícia Universidade Católica do Rio Grande do Sul, Porto Alegre, RS.

Lukoschek, V., K. J. Scott Keogh, and J. C. Avise. 2012. Evaluating fossil calibrations for dating phylogenies in light of rates of molecular evolution: a comparison of three approaches. Syst. Biol. 61:22–43

López-Fernández, H., R. L. Honeycutt, and K. O. Winemiller. 2005. Molecular phylogeny and evidence for an adaptive radiation of geophagine cichlids

from South America (Perciformes: Labroidei). Mol. Phylogenet. Evol. 34:227–244.

López-Fernández, H., K. O. Winemiller, and R. L. Honeycutt. 2010. Multilocus phylogeny and rapid radiations in Neotropical cichlid fishes (Perciformes: Cichlidae: Cichlinae). Mol. Phylogenet. Evol. 55:1070–1086.

López-Fernández, H., K. O. Winemiller, C. G. Montaña, and R. L. Honeycutt. 2012. Diet-morphology correlations in the radiation of South American geophagine cichlids (Perciformes: Cichlidae: Cichlinae). PLoS ONE 7:e33997.

Losos, J. 2010. Adaptive radiation, ecological opportunity, and evolutionary determinism. Am. Nat. 175:623–639.

Losos, J. B. 2009. Lizards in an evolutionary tree. Ecology and adaptive radiation of anoles. Univ. of California Press, Berkeley, CA.

Losos, J. B., and D. L. Mahler. 2010. Adaptive radiation: the interaction of ecological opportunity, adaptation, and speciation. Pp. 381–420 *in* M. A. Bell, D. J. Futuyma, W. F. Eanes, and J. S. Levinton, eds. Evolution since Darwin: The first 150 years. Sinauer Associates, Sunderland, MA.

Lundberg, J. G. 1993. African-South American freshwater fish clades and continental drift: problems with a paradigm. Pp. 156–199 *in* P. Goldblatt, ed. Biological relationships between Africa and South America. Yale Univ. Press, New Haven.

Mahler, D. L., L. J. Revell, R. E. Glor, and J. B. Losos. 2010. Ecological opportunity and the rate of morphological evolution in the diversification of greater Antillean Anoles. Evolution 64:2731–2745.

Malabarba, M., and L. Malabarba. 2008. A new cichlid *Tremembichthys garciae* (Acctinopterygii, Perciformes) from the Eocene-Oligicene of eastern Brazil. Rev. Bras. Paleontol. 11:59–68.

Malabarba, M. C., M. LR, and C. del Papa. 2010. *Gymnogeophagus eocenicus* n. sp. (Perciformes: Cichlidae), and Eocene cichlid from the lumbrera formation in Argentina. J. Vert. Paleont. 30:341–350.

McPeek, M. 1995. Testing hypotheses about evolutionary change on single branches of a phylogeny using evolutionary contrasts. Am. Nat. 45:686–703.

Montana, C. G., and K. O. Winemiller. 2010. Local-scale habitat influences morphological diversity of species assemblages of cichlid fishes in a tropical floodplain river. Ecol. Freshwat. Fish 19:216–227.

Murray, A. M. 2001. The oldest fossil cichlids (Teleostei : Perciformes): indication of a 45 million-year-old species flock. Proc. R. Soc. Lond. B 268:679–684.

Near, T. J., R. I. Eytan, A. Dornburg, K. L. Kuhn, J. A. Moore, M. P. Davis, P. C. Wainwright, M. Friedman, and W. L. Smith. 2012. Resolution of ray-finned fish phylogeny and timing of diversification. Proc. Nat. Acad. Sci. USA 109:13698–13703.

Paradis, E., J. Claude, and K. Strimmer. 2004. APE: Analyses of phylogenetics and evolution in R language. Bioinformatics 20:289–290.

Parham, J. F., P. C. J. Donoghue, C. J. Bell, T. D. Calway, J. J. Head, P. A. Holroyd, J. G. Inoue, R. B. Irmis, W. G. Joyce, D. T. Ksepka, et al. 2012. Best practices for justifying fossil calibrations. Syst. Biol. 61:346–359.

Pybus, O., and P. Harvey. 2000. Testing macro-evolutionary models using incomplete molecular phylogenies. Proc. R. Soc. Lond. B 267:2267–2272.

Rabinowitz, P., M. Coffin, and D. Falvey. 1983. The separation of Madagascar and Africa. Science 220:67–69.

Rabosky, D. L. 2009a. Ecological limits on clade diversification in higher taxa. Amer. Nat. 173:662–674.

———. 2009b. Ecological limits and diversification rate: Alternative paradigms to explain the variation in species richness among clades and regions. Ecol. Lett. 12:735–743.

Rabosky, D. L., and I. J. Lovette. 2008. Explosive evolutionary radiations: decreasing speciation or increasing extinction through time? Evolution 62:1866–1875.

Reis, R., S. Kullander, and C. Ferraris Jr. 2003. Check list of the freshwater fishes of South and Central America. Pontifícia Universidade Católica do Rio Grande do Sul, Porto Alegre, RS.

Revell, L. 2008. On the analysis of evolutionary change along single branches in a phylogeny. Am. Nat. 172:140–147.

———. 2009. Size-correction and principal components for interspecific comparative studies. Evolution 63:3258–3268.

———. 2012. Phytools: an R package for phylogenetic comparative biology (and other things). Method. Ecol. Evol. 3:217–223.

Revell, L., L. Harmon, R. B. Langerhans, and J. Kolbe. 2007. A phylogenetic approach to determining the importance of constraint on phenotypic evolution in the Neotropical lizard, *Anolis cristatellus*. Evol. Ecol. Res. 9:261–282.

Santini, F., L. J. Harmon, G. Carnevale, and M. E. Alfaro. 2009. Did genome duplication drive the origin of teleosts? A comparative study of diversification in ray-finned fishes. BMC Evol. Biol. 9:194.

Schluter, D. 2000. The ecology of adaptive radiation. Oxford Univ. Press, New York, NY.

Simpson, G. 1953. The major features of evolution. Columbia Univ. Press, New York, NY.

Slater, G. J., S. A. Price, F. Santini, and M. E. Alfaro. 2010. Diversity versus disparity and the radiation of modern cetaceans. Proc. R. Soc. Lond. B 277:3097–3104.

Soria-Barreto, M., and R. Rodiles-Hernández. 2008. Spatial distribution of cichlids in Tzendales river, biosphere reserve Montes Azules, Chiapas, Mexico. Environ. Biol. Fishes 83:459–469.

Sparks, J. S. 2004. Molecular phylogeny and biogeography of the Malagasy and South Asian cichlids (Teleostei: Perciformes: Cichlidae). Mol. Phylogenet. Evol. 30:599–614.

Sparks, J. S., and W. Smith. 2004. Phylogeny and biogeography of cichlid fishes (Teleostei: Perciformes: Cichlidae). Cladistics 20:501–517.

Stiassny, M. L. J. 1991. Phylogenetic intrarelationships of the family Cichlidae: an overview. Pp. 1–35 *in* M. H. A. Keenleyside, ed. Cichlid fishes: behaviour, ecology and evolution. Chapman Hall, London.

Streelman, J., and P. D. Danley. 2003. The stages of vertebrate evolutionary radiation. Trends Ecol. Evol. 18:126–131.

Takahashi, T., and S. Koblmüller. 2011. The adaptive radiation of cichlid fish in lake Tanganyika: a morphological perspective. Intl. J. Evol. Biol. doi: 10.4061/2011/620754.

Verheyen, E., W. Salzburger, J. Snoeks, and A. Meyer. 2003. Origin of the superflock of cichlid fishes from Lake Victoria, East Africa. Science 300:325–329.

Wainwright, P., L. Ferry-Graham, T. Waltzek, A. Carroll, C. Hulsey, and J. Grubich. 2001. Evaluating the use of ram and suction during prey capture by cichlid fishes. J. Exp. Biol. 204:3039–3051.

Wainwright, P. C., W. L. Smith, S. A. Price, K. L. Tang, J. S. Sparks, L. A. Ferry, K. L. Kuhn, R. I. Eytan, and T. J. Near. 2012. The evolution of pharyngognathy: a phylogenetic and functional appraisal of the pharyngeal jaw key innovation in labroid fishes and beyond. Syst. Biol. 61:1001–1027.

Webb, P. 1982. Locomotor patterns in the evolution of actinopterygian fishes. Amer. Zool. 22:329–342.

Webb, P., G. LaLiberte, and A. J. Schrank. 1996. Does body and fin form affect the maneuverability of fish traversing vertical and horizontal slits? Environ. Biol. Fishes 46:7–14.

Willis, S. C., K. O. Winemiller, and H. López-Fernández. 2005. Habitat structural complexity and morphological diversity of fish assemblages in a neotropical floodplain river. Oecologia 142:284–295.

Winemiller, K. O., L. C. Kelso-Winemiller, and A. L. Brenkert. 1995. Ecomorphological diversification and convergence in fluvial cichlid fishes. Environ. Biol. Fishes 44:235–261.

Winemiller, K. O., H. López-Fernández, D. C. Taphorn, L. G. Nico, and A. B. Duque. 2008. Fish assemblages of the Casiquiare River, a corridor and zoogeographical filter for dispersal between the Orinoco and Amazon basins. J. Biogeogr. 35:1551–1563.

Winemiller, K. O., D. C. Taphorn, and A. Barbarino-Duque. 1997. Ecology of *Cichla* (Cichlidae) in two blackwater rivers of southern Venezuela. Copeia 1997:690–696.

Yoder, J. B., E. Clancey, S. Des Roches, J. M. Eastman, L. Gentry, W. Godsoe, T. J. Hagey, D. Jochimsen, B. P. Oswald, J. Robertson, et al. 2010. Ecological opportunity and the origin of adaptive radiations. J. Evol. Biol. 23:1581–1596.

Zuanon, J. 1999. História natural da ictiofauna de corredeiras do rio Xingu, na região de Altamira, Pará. Unpublished thesis. Universidade Estadual de Campinas, Campinas, SP.

Associate Editor: T. Streelman

Supporting Information

Additional Supporting Information may be found in the online version of this article at the publisher's website:

Appendix S1. Fossil calibration procedures.

Appendix S2. Table of posterior probability, age, and age ranges obtained for each of the nodes in the chronogram depicted in Fig. 1. Numbers follow node labels given in Fig. 1.